

# Sepiolite as a deodorant material: an ESR study of its properties

HISASHI UEDA

*National Chemical Laboratory for Industry, Higashi 1-1 Tsukubashi, Ibaraki 305, Japan*

MAKIYO HAMAYOSHI

*Ujiden Kagaku Co., Sanbashidori 5-7-34, Kochishi, Kochi 780, Japan*

Sepiolite, a Mg silicate, is used as a deodorant because of its strong adsorbing power. However, the principle by which sepiolite adsorbs gases is not known well. The present authors have tried to analyse this principle as a change of paramagnetic species in the crystal surfaces of sepiolite. After heat-processing sepiolite at the temperatures 150, 550 and 750°C, the concentration change of paramagnetic species was observed using NH<sub>3</sub>, air, or vacuum as atmospheric environment of sepiolite. The results indicate that, in the absence of zeolitic water, relatively high concentrations of Mn<sup>2+</sup> and (Mg<sup>2+</sup>)<sub>n</sub><sup>-</sup> are observed, which are destroyed with NH<sub>3</sub> or water. A multi-line ESR spectrum has been found and is attributed to (Mg<sup>2+</sup>)<sub>n</sub><sup>-</sup> ion which is an entire crystal lattice plane forming a big molecular orbital. The results and an analysis of it seem to indicate that a gas molecule is adsorbed to a crystal plane of sepiolite due to its "free spin" holding nature. This phenomenon may be called "spin adsorption". There should be many more cases in which gas adsorption from the gas phase to the solid phase is controlled by the free-spin holding nature of the solid surface. For such cases the ESR method seems to be a quite powerful and proper technique.

## 1. Introduction

There are two types of atmospheric pollution in the environment of human beings. One type is known as global pollution, and another is known as local pollution. Among local pollution, the presence of bad-smelling substances is often encountered and it is desired to replace them with clean air. For this purpose, deodorant materials are often needed. The polluting substances which originate from human or animal bodies are mostly reducing substances such as amines or mercaptanes. Therefore, if we can find some deodorant materials which can remove these types of compound from the atmosphere, a more pleasant living environment can be established.

Sepiolite has strong adsorption power and also it has a plastic nature in the bulk state, and therefore has various interesting applications. The occurrence and general properties of sepiolite have been described in the literature [1-5]. The temperature dependence and thermal analysis data have been given [6-8]. Several cases of gas absorption by sepiolite and attapulgite have also been shown [9]. It has three fundamental properties: adsorbability, rheological property, and solidification by drying. The absorption capacity is the basis for the deodorant use of the mineral. However, the chemistry of the adsorption phenomenon itself has not been studied much with sepiolite. Adsorption may be classified into two categories. One is that in which chemical bonds change during the adsorption process,

the chemisorption process. The other is that in which no chemical bonds change during the adsorption process, the physisorption process. Sepiolite has some tunnel-like structure in which some molecules can be trapped [10]. In order to see the change of chemical bonds during the adsorption of NH<sub>3</sub> by sepiolite, an ESR study of sepiolite during the adsorption of NH<sub>3</sub> has been tried. The results have indicated that unexpectedly large change of electron spin occur during the adsorption process.

## 2. Experimental procedure

Sepiolite, originally produced in Turkey, was given by Ujiden Chemical Ind., Ltd. Ammonia gas was obtained from aqueous ammonium hydroxide by repeated vacuum distillation at 0°C. This ammonia gas was stored in a reservoir attached to the vacuum line by which the ESR sample system was evacuated or fed with gases. Sepiolite has various forms of water molecules bonded to it if it is not dried with particular care. Therefore it is expected that removal of these water molecules from sepiolite affects the adsorption of NH<sub>3</sub> by this mineral. To find the effects of water molecules on NH<sub>3</sub> adsorption, four samples were prepared and were used for measurements:

1. The original sepiolite as received.
2. Treated in air at 150°C for 3 h. This sample will be referred to as S-150.

3. Treated in air at 550°C for 3 h. This sample will be referred to as S-550.

4. Treated in air at 750°C for 3 h, to be referred to as S-750.

0.25 g of one of the above four samples was placed in the sample tube connected to the vacuum line already described. Evacuation, gas introduction or evacuation again were carried out with this sample and the resulting changes in the ESR spectra were observed and recorded. Evacuation were made to the extent of  $10^{-4}$  torr. ESR spectra were recorded by a JES-ME3X spectrometer (Jeol). A magnetic field modulation frequency of 100 kHz and a microwave frequency of 9.445 GHz, input microwave power of 1 mW, and magnetic field modulation widths of 0.05 mT (in the case of  $Mn^{2+}$  h.f.s. spectra) and 0.5 mT (in the case of  $Mn^{2+}$  and  $Mg^{+}$  spectra) were employed. The ammonia gas pressure was measured with a mercury tube manometer attached to the vacuum line. Thermal analyses of the sample were made with a thermal analyser (Ver 2.20 of Rigaku Denki Co.) employing the thermogravimetry (TG) and differential thermal analysis (DTA) mode.

### 3. Results

Fig. 1 indicates the results of thermal analysis of sepiolite and their relation to the thermal treatments given to sepiolite samples. The thermal treatment at 150°C removes zeolitic water and adsorbed water. The thermal treatment at 550°C removes some 50% of the bonded water. The thermal treatment at 750°C removes even the  $OH^{-}$  groups which are bonded to Si atoms. When an untreated sepiolite sample was evacuated at room temperature (RT), it gave paramagnetic species as shown in Figs 2 and 3. X-band ESR spectra reveal the presence of several absorptions. One has peaks of the first derivative curve at  $\sim 50, 80$  and 155 mT, named as A, B and C, respectively. The second is a multi-line absorption appearing in the magnetic field region between 100 and 650 mT. The third is the  $Mn^{2+}$  h.f.s. lines appearing near 336 mT. The fourth is a broad absorption existing in the magnetic field region of 100–600 mT. Absorption near

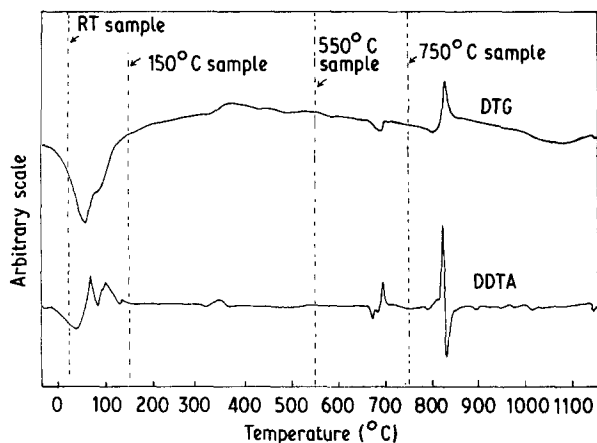


Figure 1 Relation between the thermal analysis and thermal treatment of sepiolite samples used.

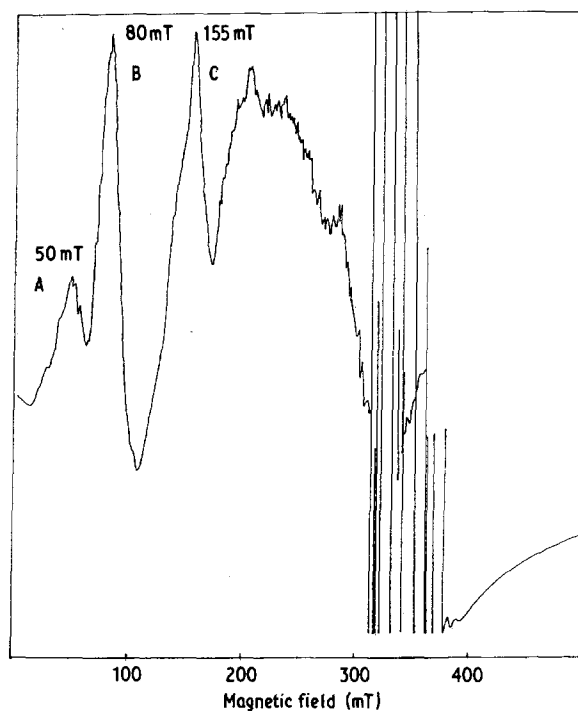


Figure 2 ESR spectrum (9.450 GHz) of the species A, B, C and  $Mn^{2+}$  which appear in the magnetic field region 0–500 mT, obtained from sepiolite without preliminary thermal treatment.

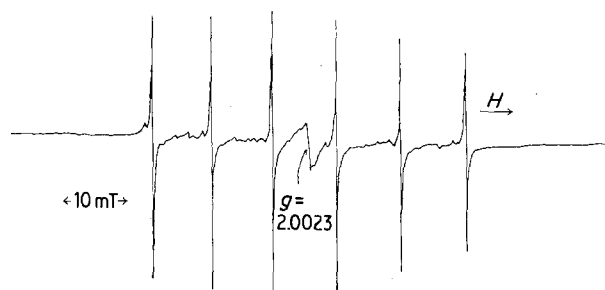


Figure 3 ESR spectrum (9.440 GHz) obtained from thermally untreated (but in a vacuum) sepiolite in the magnetic field region 286–386 mT.

$g = 2.0023$  is also observed. The ESR spectrum in the  $250 \pm 250$  mT region is shown in Fig. 2. The ESR spectrum in the  $336 \pm 50$  mT region is shown in Fig. 3.

#### 3.1. $g = 2.0023$ absorption

The change of  $g = 2.0023$  intensity is as shown in Table I. In the table Air-1 signifies the relative intensity value observed when the sample was cooled in the air after thermal treatment. EV-1 signifies the relative ESR intensity value observed when the sample was evacuated to  $10^{-4}$  torr after measuring the Air-1 value. “ $NH_3$ ” signifies the relative ESR intensity value observed when some 40 torr of  $NH_3$  gas was introduced into the sample after measuring the EV-1 value. A further evacuation of the “ $NH_3$ ” sample for 25 min gave the value EV-2. An introduction of air (700 torr) gave the result Air-2. An evacuation of the Air-2 specimen to  $10^{-4}$  torr gave the result EV-3. It seems that these results have shown that this paramagnetic

TABLE I Relative intensities of  $g = 2.0023$  ESR lines

Heat treatment temperature (°C)	Sample					
	Air-1	EV-1	NH <sub>3</sub>	EV-2	Air-2	EV-3
None	1.0	13.0	7.3	18.3	18.3	18.3
150	8.3	18.3	11.3	19.3	19.3	36.0
550	114	112	80	108	108	111
750	8.7	6.3	6.3	5.7	9.0	7.7

species increases when the weakly and strongly bonded water molecules are removed; but if OH<sup>-</sup> is removed, the intensity of this species is decreased. It will also be seen that NH<sub>3</sub> decreases the intensity of this absorption.

### 3.2. ESR absorption in the 100–650 mT region

ESR absorption consisting of many lines and appearing in the magnetic field region 100–650 mT has been observed in this work for the first time. It seems that the number of coupling nuclei is quite large and the spin density may have positive and negative values. The relative intensity values in the region 240–260 mT are as shown in Table II. The most intense case of this absorption (observed in the sample treated at 550°C, EV-1 spectrum) and the spectrum observed after NH<sub>3</sub> introduction to this EV-1 sample are shown in Fig. 4. It will be seen that the multi-line ESR absorption which has been intensified by the EV-1 procedure has again become weak by the introduction of NH<sub>3</sub> gas. The values in Tables I and II

TABLE II Relative intensities of 100–650 mT ESR lines

Heat treatment temperature (°C)	Sample					
	Air-1	EV-1	NH <sub>3</sub>	EV-2	Air-2	EV-3
None	1	17	8	27	26	30
150	6	20	22	36	34	47
550	40	48	20	37	37	41
750	1	2	1	11	5	9

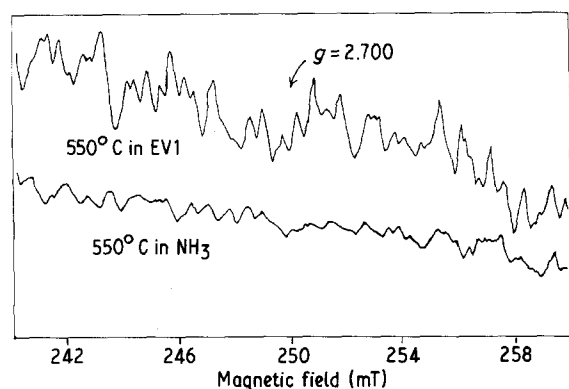


Figure 4 ESR spectra (9.448 GHz) of sepiolite, pretreated at 550°C, in NH<sub>3</sub> and in a vacuum (EV1) at 20°C, in the magnetic field region 240–260 mT.

have similar tendencies and therefore the paramagnetic species giving rise to Figs 2 and 4 are closely related species.

### 3.3. ESR absorption near 50, 80 and 155 mT

The absorption  $A$  which appears near 50 mT has a  $g$ -factor value of 13.5, which seems to indicate that this absorption is due to a metal ion which has many 3d electrons such as Co<sup>2+</sup>. The absorption near 80 mT,  $B$ , has a  $g$ -factor of 8.4, which may indicate that the corresponding paramagnetic species are Co<sup>2+</sup> or Ni<sup>2+</sup> ions. The absorption near 155 mT,  $C$ , is similar to the ESR absorption of Fe<sup>3+</sup> contained in alumina, and probably is due to Fe<sup>3+</sup>.

### 3.4. The Mn<sup>2+</sup> ESR absorption

Fig. 3 indicates the ESR absorption due to Mn<sup>2+</sup> ( $S = 5/2$ ). The line widths of these lines are not equal to each other, the line width of the third line from the lower side of magnetic field being the narrowest. This line width changes by evacuation, NH<sub>3</sub> introduction, re-evacuation, air introduction, and evacuation for the third time. The results obtained from four different samples (untreated sample, S-150, S-550 and S-750) are shown in Figs 5–8, respectively.

### 3.5. ESR spectrum of 750°C treated sample

As shown in Fig. 8, the changes of ESR spectra, when NH<sub>3</sub> is introduced or the sample is evacuated, are different in the S-750 sample from those of S-150 and S-550. The ESR spectrum due to Mn<sup>2+</sup> obtained from S-750 sample is shown in Fig. 9. It indicates that the crystalline structure of sepiolite has been changed by heat treatment at 750°C. The total intensity has decreased considerably from that of the Fig. 3 spectrum, and the coupling constant values,  $A$ , and  $g$ -factor values have changed. In Fig. 3,  $A = 0.0090$  cm<sup>-1</sup> and  $g = 2.0063$  while in Fig. 9,  $A_1 = 0.0092$ ,  $g_1 = 2.0083$ ,

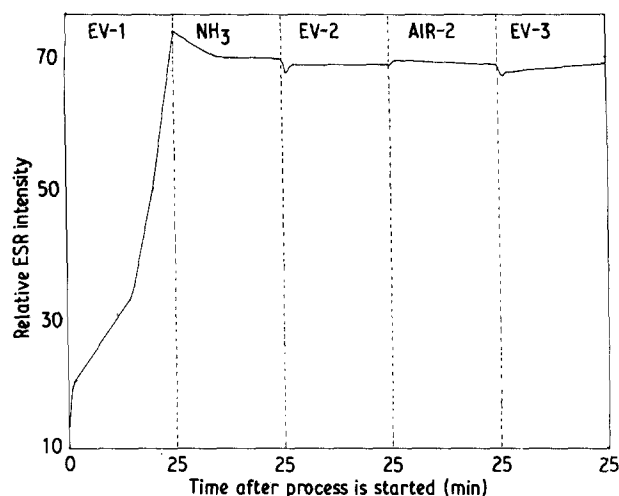


Figure 5 Intensity variation of one of the ESR lines from Mn<sup>2+</sup> when the atmosphere was changed. EV-1: in a vacuum of 10<sup>-4</sup> torr, NH<sub>3</sub>: in NH<sub>3</sub> gas of 40 torr, EV-2: evacuated to 10<sup>-4</sup> torr again, AIR-2: air (~ 700 torr) introduced, EV-3: evacuated to 10<sup>-4</sup> torr for the third time. The sample used was not thermally treated.

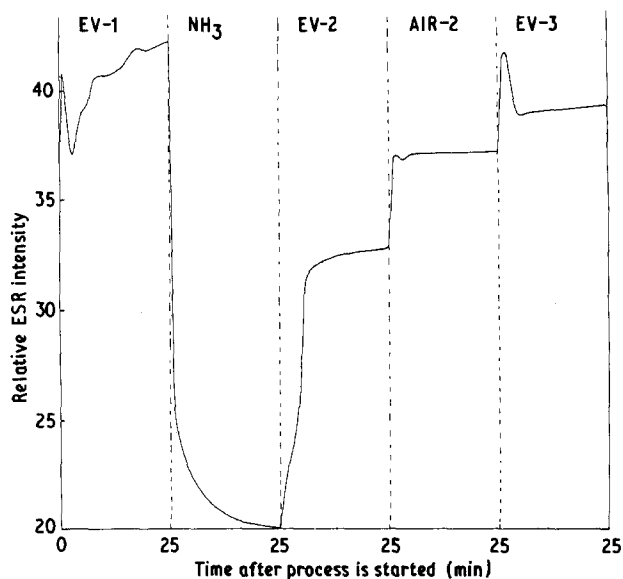


Figure 6 The sample used was treated in air at 150°C for 3 h. Other conditions are the same as those in Fig. 5.

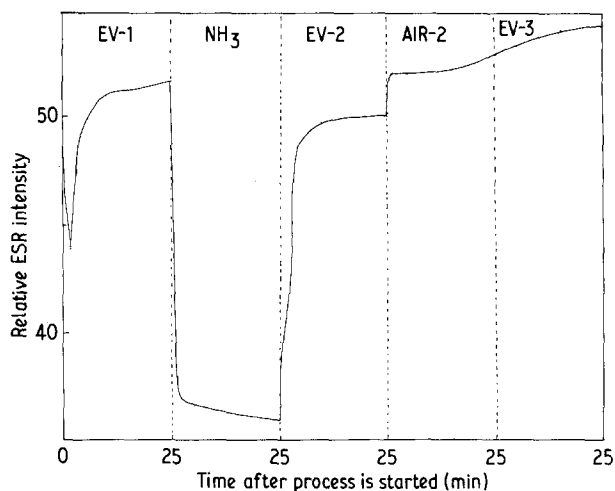


Figure 7 The sample used was treated in air at 550°C for 3 h. Other conditions are the same as those in Fig. 5.

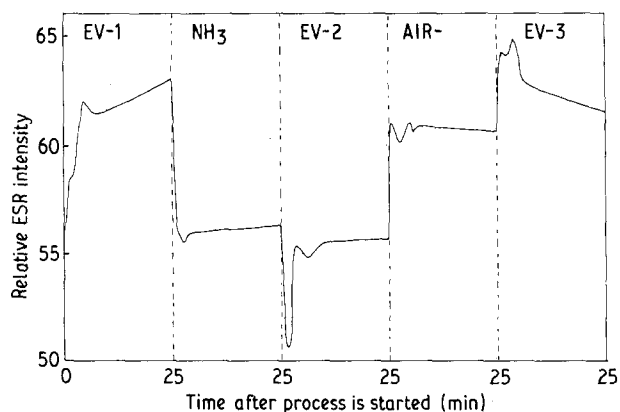


Figure 8 The sample used was treated in air at 750°C for 3 h. Other conditions are the same as those in Fig. 5.

$A_2 = 0.0086$  and  $g_2 = 2.0056$ . This indicates that  $Mn^{2+}$ , existing as an impurity ion in the sepiolite lattice, has moved from the original site to two different sites in the lattice. It will also be noted that the

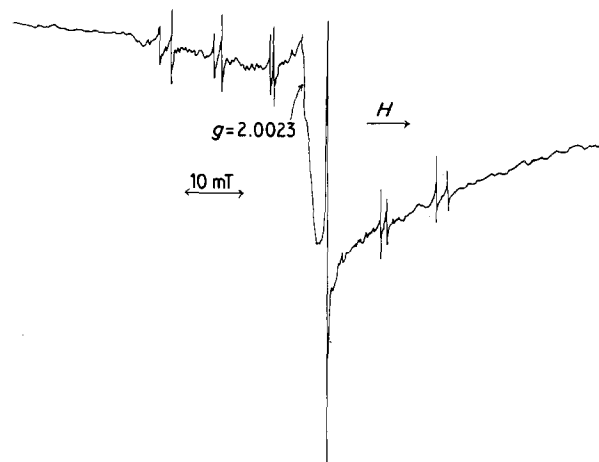


Figure 9 ESR spectrum (9.450 GHz) of sepiolite sample EV1 pre-treated at 750°C in air for 3 h. Magnetic field region 286–386 mT. The spectrum is clearly different from Fig. 3.

fourth line, counted from the lower field side, is some 3.2 times as strong as the value expected from other lines.

### 3.6. Absorption capacity of $NH_3$ gas

Table III shows the amount of  $NH_3$  gas absorbed in 25 min by sepiolite thermally treated at different temperatures. It indicates that the sepiolite from which adsorbed water and zeolitic water have been removed by thermal treatment adsorbs  $NH_3$  gas with the fastest rate.

## 4. Discussion

### 4.1. Paramagnetic species related to $NH_3$ adsorption

The ESR absorption shown in Tables I and II and in Figs 4–8, namely  $g = 2.0023$  absorption, multi-line absorption (a part of it in the field region 240–260 mT has been shown) and  $Mn^{2+}$  absorption, all decreased their intensities when  $NH_3$  was introduced into sepiolite specimens. On the other hand, evacuation intensified these absorptions, probably by removing the adsorbed water molecules. These effects of water and  $NH_3$  molecules indicate that electron-donating molecules will cause some change to the paramagnetic species in sepiolite which exist in the crystal plane in which there are net positive electric charges.

The ESR absorption appearing at  $g = 2.0023$  is identical in shape with the ESR spectrum obtained from an MgO sample reduced in an  $H_2$  atmosphere at 400°C. This MgO spectrum was assigned to an assembly of  $Mg^+$  ions produced from  $Mg^{2+}$  ions which were located in positions where reduction occurs relatively easily. The multi-line ESR spectrum, only a part of which has been shown in Fig. 4, may be concluded to be due to  $Mg^+$  ions which are well dispersed on the layer crystal plane of sepiolite.

The reason for this is as follows. Firstly it is not from a cluster of  $Mn^{2+}$  ions. As the ESR spectrum of  $Mn^{2+}$  is as shown in Fig. 3, they should be well dispersed in the sepiolite crystal. If so, the unpaired electron spin cannot be distributed to many Mn ions.

Other ionic species which have a nuclear spin magnetic moment are derived from Mg only. Therefore, it will be necessary to examine the structure of sepiolite to see if it can have some unpaired electron system which involves many  $Mg^{2+}$  ions.

#### 4.2. A possible molecular orbital of $Mg^{2+}$ in sepiolite

As to the structure of sepiolite, Brauner and Preisinger [10] and Nagy and Bradley [11] have done detailed research. According to them, the crystalline  $b$ - $c$  plane is as shown in Fig. 10. In addition to those water molecules and  $Mg^+$  ions which can be seen on the  $b$ - $c$

plane, some additional water molecules and  $Mg^+$  ions which can be seen on the  $a$ - $b$  plane have been added to Fig. 10. Fig. 10 shows that there are  $Mg^{2+}$  planes and  $O^-$  and  $OH^-$  planes which are parallel to the  $a$ - $b$  plane; these are denoted as  $\Pi_{Mg}$  and  $\Pi_O$ , respectively.  $Mn^{2+}$  is supposed to replace some of  $Mg^{2+}$  ions in  $\Pi_{Mg}$ . The  $Mg^{2+}$ - $Mg^{2+}$  distance in Fig. 10 is 0.1510 nm. This distance is almost comparable to the C-C distance of 0.1397 nm in a benzene molecule. Therefore, a molecular orbital consisting of  $Mg^{2+}$ - $Mg^{2+}$ ---is possible if the planarity of the arrangement is guaranteed.

$\Pi_O/\Pi_{Mg}/\Pi_O$ , a three-layer section in the middle of Fig. 10, may be magnified as shown in Fig. 11. There

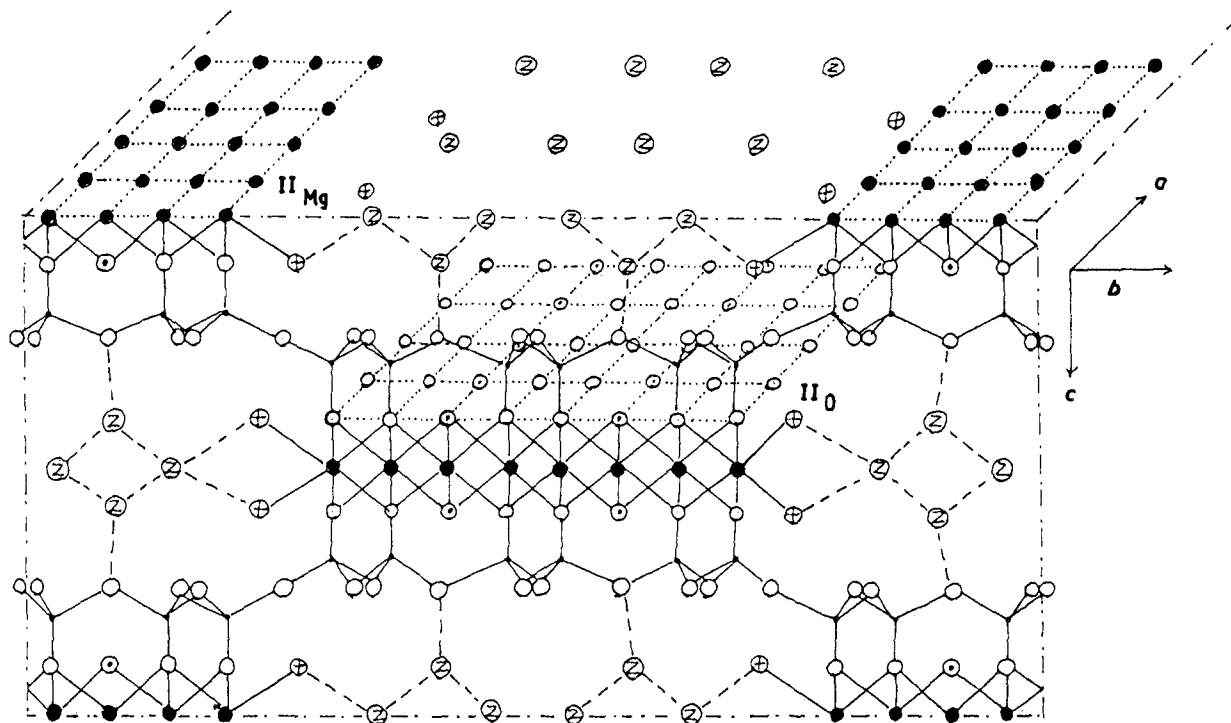


Figure 10 Sepiolite crystal viewed from  $a$ -axis direction. (●) Si, (●) Mg, (○) O, (⊙) OH, (⊕)  $H_2O$  (cryst.), (Z)  $H_2O$  (Zeol).

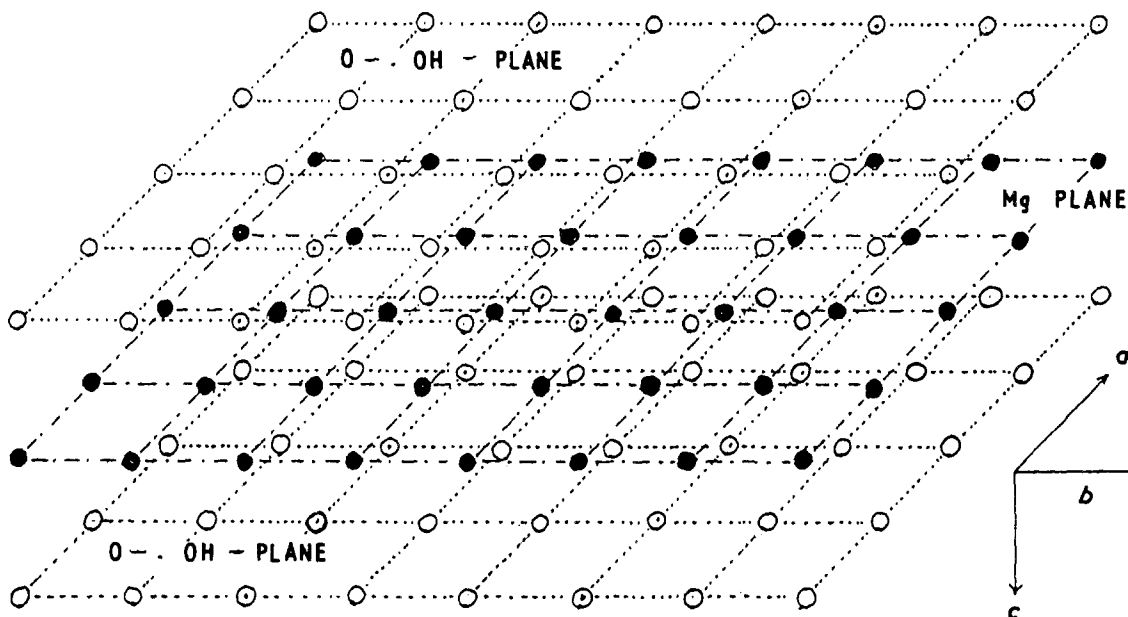


Figure 11 The central part of Fig. 10 where  $Mg^{2+}$  forming an Mg-plane,  $\Pi_{Mg}$ , is sandwiched between oxygen (or  $OH^-$ ) planes,  $\Pi_O$ . (○) O, (⊙) OH, (●) Mg.

are three stable isotopes of Mg, namely  $^{24}\text{Mg}$ ,  $^{25}\text{Mg}$  and  $^{26}\text{Mg}$ , natural abundances of which are 78.60, 10.11 and 11.29% respectively. Only  $^{25}\text{Mg}$  has nuclear spin magnetic momentum, and the quantum number is  $I = 5/2$ . If the coupling constant of a  $^{25}\text{Mg}$  nucleus is written as  $A$ , the ESR absorption lines will appear at  $\pm A/2$ ,  $\pm 3A/2$  and  $\pm 5A/2$  distances with relative intensities of 1.87 if the central strongest line is counted as intensity = 100. As shown in Fig. 11, if we assume a total spin density of 1.0 is distributed on an array of  $8 \times 5 = 40$  Mg ions, the spin density having both positive and negative signs, one of the possible solutions will be  $\rho_i = +0.5$  at 21 Mg orbits and  $\rho_i = -0.5$  at 19 Mg orbits which then gives  $\sum \rho_i = 1.0$ . Therefore, in a structural model in which the lattice plane in Fig. 11 constitutes a molecular orbital and a total spin density of  $\sum \rho_i = 1.0$  is distributed over all the Mg ions in the plane, an ESR spectrum having a strong central line and some 400 weak satellite lines may be observed. Therefore, the ESR spectrum, a part of which has been shown in Fig. 4, can only be interpreted by the structural model in Fig. 11. As shown by Fig. 11,  $\text{O}^-$  (this may more properly be written as  $\text{O}^{2-}$ , but O is a part of the  $(\text{SiO}_4)^{4-}$  structure and so the formal charge on oxygen should be  $-1$ ) [4] and  $\text{OH}^-$  are also arranged on the same plane. Therefore, this  $\text{O}^-$ - $\text{OH}^-$  plane,  $\Pi_0$ , may also be able to accommodate a molecular orbital.

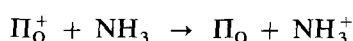
As to the S-750 sample, it may be said that  $\text{OH}^-$  ions may escape from the  $\Pi_0$  plane by the heat treatment at  $750^\circ\text{C}$ , and as a result an  $\text{Mg}^{2+}$  ion located right above (or below) this  $\text{OH}^-$  ion may shift its position in the up (or down) direction. If an impurity  $\text{Mn}^{2+}$  ion is in this position, its ESR spectrum will reflect this deviation from the original position, having a lower symmetry. Such a change will break the planar arrangement of  $\text{Mg}^{2+}$  ions and therefore the intensity of the Fig. 9 spectrum should become weak with this specimen. In Table II, the ESR intensities of the S-750 sample actually are weak.

#### 4.3. The adsorption of $\text{NH}_3$ and intensity of ESR absorption

As  $\Pi_0$  and  $\Pi_{\text{Mg}}$  form a three-layer structure,  $\Pi_0/\Pi_{\text{Mg}}/\Pi_0$ , it may be possible that a charge transfer from the  $\Pi_0$  plane to the  $\Pi_{\text{Mg}}$  plane takes place



which is actually a polarization between two crystal planes. In the case of an S-550 sample, almost no electron donor is coordinated to the  $\Pi_0^+$  plane, and so only the ESR spectrum of  $\Pi_{\text{Mg}}^-$  should be observed in a vacuum. Actually this is so. However, if  $\text{H}_2\text{O}$  or  $\text{NH}_3$  is adsorbed by the  $\Pi_0^+$  plane, the charge transfer



takes place and the positive charge of the  $\Pi_0^+$  plane is neutralized. The electric charge on  $\Pi_{\text{Mg}}^-$  is, so to speak, induced by the positive charge of two  $\Pi_0^+$  planes existing above and below this layer. So, if the positive charge in the  $\Pi_0^+$  plane is neutralized, the electrostatic potential of the  $\Pi_{\text{Mg}}^-$  plane is raised to some extent. Then the extra electron or the unpaired electron is

excited to the conduction band or set free to move around, finally to be trapped by a hole such as  $\text{Mn}^{3+}$  or  $\text{NH}_3^+$ . Thus the ESR signal from  $\Pi_{\text{Mg}}^-$  decays. In another words,  $\text{NH}_3$  or  $\text{H}_2\text{O}$  molecules, though they do not come in contact with  $\Pi_{\text{Mg}}^-$  directly, cancel the electric charge in  $\Pi_{\text{Mg}}^-$  by neutralizing the positive charge in the  $\Pi_0^+$  plane. Thus the magnetic properties of  $(\text{Mg}^{2+})_{40}$  are strongly affected by  $\text{NH}_3$  or  $\text{H}_2\text{O}$ .

#### 4.4. Spin adsorption

Generally speaking, when a gas molecule is adsorbed by a solid surface, simple physisorption will be taking place in most of them. However, in the process taking place in sepiolite, there are polarization processes among crystal planes such as  $\Pi_{\text{Mg}}^- + \Pi_0 \rightarrow \Pi_{\text{Mg}}^- + \Pi_0^+$ . Gas adsorption takes place in a form to cancel the electric charge thus created by plane-to-plane polarization. This process may therefore, be termed "spin adsorption". Since the plane system ( $\Pi_{\text{Mg}}^- + \Pi_0^+$ ) can be considered to be a stable free-radical system, there will be other spin adsorption phenomena taking place in different types of stable free-radical system.

#### 5. Conclusion

It has been shown that sepiolite, a magnesium silicate mineral, having a strong absorption capacity for gases, and having already been used as a deodorant material, changes its electron spin states when it adsorbs  $\text{NH}_3$ . Although the  $\text{Mg}^{2+}$  layers are not directly accessible to  $\text{NH}_3$  and other gases, its  $\text{OH}^-$ - $\text{O}^-$  layers, having a net positive charge, are accessible to  $\text{NH}_3$  and the net positive charge held by  $\text{OH}^-$ - $\text{O}^-$  layers are neutralized by  $\text{NH}_3$ . It is this neutralization process that cancels the positive charge on the  $\text{Mg}^{2+}$  plane because the positive charge has been induced by the negative charge on the  $\text{OH}^-$ - $\text{O}^-$  plane. These facts indicate that when analysing the deodorant mechanism of silicate minerals and other deodorant materials, ESR studies in which the change of electron spin states can be observed will furnish essential information.

#### References

1. H. F. MARK, (ed.), "Kirk-Othmer Encyclopedia of Chemical Technology", 3rd Edn, Vol. 6 (Wiley, New York, 1979) p. 202.
2. R. E. GRIM, "Clay Mineralogy" (McGraw-Hill, New York, 1968) p. 44.
3. T. KUDO and S. SHIMODA, "Developments in Sedimentology" (Kodansha, Tokyo, 1978) pp. 66, 69.
4. R. W. GRIMSHAW, "The Chemistry and Physics of Clay" (Ernst Benn, London, 1971) pp. 124, 968.
5. E. INGERSON (ed.), "Clays and Clay Minerals" (Pergamon, Oxford, 1962) p. 592.
6. G. MIGEON, *Bull. Soc. Franc. Mineral.* **59** (1936) 6.
7. H. NAGATA, S. SHIMODA and T. KUDO, *Clays & Clay Miner.* **22** (1974) 285.
8. J. L. M. VIVALDI and J. L. GONZALEZ, "Clays and Clay Minerals" (Pergamon, Oxford, 1962) p. 596.
9. R. M. BARRER, N. MACKENZIE and D. M. McLEOD, *J. Phys. Chem.* **58** (1954) 568.
10. K. BRAUNER and A. PREISINGER, *Tschermaks Miner. Petrogr. Mitt.* **6** (1956) 120.
11. B. NAGY and W. F. BRADLEY, *Amer. Miner.* **40** (1955) 885.

Received 20 May

and accepted 26 September 1991